Spinal Cord Injury: Neuropathology well away from the lesion contributes to dysfunction

Undergraduate Research Honors Thesis

Presented in partial fulfillment of the requirement for graduation *with honors research distinction* in Neuroscience in the undergraduate colleges of The Ohio State University

Molly O'Shea

PI: D. M. Basso, PT, Ed. D., Associate Director, School of Health and Rehabilitation Sciences
Timothy D. Faw, PT, DPT, NCS, Neuroscience Graduate Studies Program
Lesley Fisher, Center for Brain and Spinal Cord Repair
Samantha Kerr, Center for Brain and Spinal Cord Repair
Rochelle Deibert, Center for Brain and Spinal Cord Repair
Kathleen Kisseberth, The Ohio State University College of Arts and Sciences

Abstract:
Spinal cord injury (SCI) results in sensory and motor dysfunction and ultimately physical, psychological, and financial burden. Unfortunately, the cure for SCI remains elusive and intensive neurorehabilitation produces only modest functional gains. The most abundant cells in the CNS, astrocytes, are essential to neuronal function through bidirectional communication, support, and maintenance of the blood-brain / blood-spinal cord barrier (BBB/BSCB). Studies of the injury epicenter have identified activation and proliferation of astrocytes in the production of a glial scar as an essential component of the innate post-injury response. While this response is well characterized, the role of astrocytes in remote regions is controversial and less understood. Studies suggest a decreasing gradient of astrocyte reactivity moving away from the epicenter, however studies extending into the lumbar cord display conflicting results. To determine the remote astrocytic response, we examined the time course of astrocyte dysfunction in the intermediate grey matter of the lumbar spinal cord at 7, 14, 21, and 42 days post injury (dpi) using C56BL/6 mice after a moderate (75 kilodyne) midthoracic contusion injury. We examined the BSCB in detail by labeling vasculature with tomato lectin, astrocytes with GFAP, and their interface with aquaporin-4. Additionally, we used the cell adhesion molecule, ICAM-1, to determine the presence of active trafficking of peripheral cells into the CNS as well as Iba-1 to examine microglia/macrophage morphology. GFAP was seen to be significantly upregulated at 7 dpi and remained slightly elevated through 42 dpi. Microglia/macrophages displayed a reactive phenotype and increased expression through 42 dpi with biphasic peaks at 7 and 21 dpi. ICAM-1 showed slight increases at 14 dpi, indicating active trafficking of peripheral immune cells into the cord, and AQP4 was localized to the vasculature at all time points with an apparent increase in co-labeling at 7 dpi. These results provide valuable insight into astrocyte dysfunction in key locomotor regions essential for functional recovery following SCI as well as focus for future research to help improve the benefits of activity based therapies like treadmill training.

Introduction:

In the United States alone, there are an estimated 276,000 people living with spinal cord injuries (SCI) and 12,500 new cases yearly (NSCISC). The physical and emotional toll that an SCI exacts on an individual is extreme not only for those affected, but their family and friends as well. While pharmacological interventions as well as activity-based therapies have been extensively studied for years, interventions capable of returning patients to their pre-injury normal function remain elusive. This may be due in part to the complex nature of SCI and the many areas that remain poorly understood. While the injury response has been well characterized at the epicenter, it is important to understand the remote microenvironment caudal to the lesion, where locomotor central pattern generators (CPGs) are located (Kiarulff, 1996; Ahn, et al., 2006).

Of increasing interest to our lab is the response of astrocytes in areas associated with locomotor functioning, since this remains unknown. The intermediate grey matter of the lumbar spinal cord contains CPGs, which are involved in producing rhythmic outputs at the level of the cord. CPGs have been localized partially to lamina VII of the lumbar cord by investigations of c-fos positive cells. This study found a great number of c-fos positive cells in lamina VII (Ahn et al., 2006). Lesion studies have also shown localization of CPG networks to the intermediate grey matter of the lumbar spinal cord (Kjaerulff, 1996). Behavioral treatments like treadmill- training target CPGs. This makes the intermediate zone an important area to focus on to reduce this secondary inflammatory response that could improve the impact of these therapies.

Astrocytes are among the most abundant cells in the CNS. Astrocytes are essential to formation and maintenance of the blood brain barrier (BBB) / blood spinal cord barrier (BSCB). They are also involved in regulation of blood flow through their numerous contacts with blood vessels, homeostasis of fluid and ions, BBB barrier properties, and a variety of other functions (Sofroniew and Vinters, 2010). The role of astrocytes following SCI remains controversial. Some researchers suggest that therapeutic removal of reactive astrocytes would be of greatest benefit to recovery, while others argue for their positive contributions after an injury (Sofroniew and Vinters, 2010). Even with differing opinions on the role of astrocytes after SCI, many agree that they should be investigated further in order to evaluate their role.

Epicenter:

As mentioned previously, the environment surrounding the lesion epicenter at acute time points after an SCI has been extensively studied (Popovich et al., 1996; Mautes et al., 2000; Bareyre and Schwab, 2003). After an injury, through primary damage to vasculature, peripheral immune cells are able to enter into the previously isolated central nervous system (CNS) and greatly impact the spinal cord structure and function. This primary injury leads to entrance of neutrophils and T-lymphocytes into the injury site. These cells release cytokines that regulate cell-to-cell communication and produce multiple cytotoxic effects on surrounding tissues. In the acute phase of the secondary injury response, ischemic damage (Sandler and Tator, 1976) leads to increases in free radicals and excitatory neurotransmitters, and the activation of glial cells including microglia and astrocytes.

Microglia become activated and contribute to phagocytosis and pro-inflammatory cytokine production. As peripheral immune cells and macrophages are recruited into the epicenter, they contribute to a secondary wave of inflammation. This continues out to 42 days after the injury and can have a negative impact on recovery. This can also further damage vulnerable tissue around the impact site where the initial cell death occurs (Popovich and Hickey, 2001; David et al., 2014).

Activated astrocytes also express pro-inflammatory cytokines, glial fibrillary acidic protein (GFAP), and other markers of activation following SCI (Sofroniew and Vinters, 2010). Tumor necrosis factor alpha (TNFα) and interleukin-1 beta (IL-1β), contribute further to damage of tissue and induce the expression of intracellular adhesion molecule 1 (ICAM-1), which helps with trafficking of peripheral immune cells into the CNS. At acute time points following a severe contusion, astrocytes at the epicenter proliferate demonstrating overlapping of astrocytic domains, cell body hypertrophy, and glial scarring. The resulting glial scar serves as a physical and chemical barrier around the primary lesion to isolate the injury site from the rest of the spinal cord tissue. Activated astrocytes also serve to inhibit axon regeneration at the epicenter through the production of chemicals and cause cytotoxic edema through the disregulation of aquaporin water channels (Sofroniew and Vinters, 2010; Gwak et al., 2011). Over time, damage to channels and receptors persist and have been associated with the development of chronic neuropathic pain (CNP) and sensitivity of dorsal horn neurons (Bareyre and Schwab, 2003). As a result, this secondary injury response has become a prime target for pharmacological therapies (Kwon et al., 2004).

Lumbar:

Remote from the site of the lesion, in the lumbar cord, much less is known. This area is important because of its role in locomotor functioning, and has started to receive increased

scrutiny in the field. Activation of glial cells caudal to the epicenter has also been found to contribute to CNP (Detloff et al., 2008; Nesic et al., 2005). Our lab has identified activated microglia as soon as 24h after injury up to 10 segments caudal to the injury site (Detloff et al., 2008; Hansen et al., 2013). In a timecourse study, we showed increased expression of TNFα and IL1β by 7d that returned to basal levels by 35d in the dorsal horn of the lumbar cord. Interleukin 6 (IL6), also a pro-inflammatory cytokine, was found to have increased levels of expression at more chronic 21 and 35 days post injury (dpi) (Detloff et al., 2008).

There is conflicting evidence regarding whether reactive astrocytes display upregulation of GFAP at chronic time points in the lumbar cord (Detloff et al, 2008, Nesic et al, 2005). At 35d in the L5 dorsal horn, we previously found increased GFAP mRNA without a resulting increase in GFAP protein levels (Detloff et al., 2008). Nesic et al., however, found increased expression of GFAP, S100β, and Aquaporin- 4 (AQP4) that persisted to nine months after injury (Nesic et al., 2006).

Aquaporin water channels have been found to be over-expressed after SCI in the dorsal horn of the lumbar cord up to 9 months post injury. They are thought to be involved in edema and disruption of the water/ion homeostatic balance after injury (Nesic et al., 2005). In the brain, AQP4 has been implicated in cytotoxic edema, since removal of channels led to increased edema. Since these channels are localized to the endfeet of the astrocytes, it has also been postulated that they have an important role in the function of the BBB and BSCB (Francesca and Rezzani, 2010). Nesic et al. argued that this swelling of the endfeet had a negative impact on sensory dysfunction after injury, including development of central neuropathic pain. Animals that displayed CNP also showed a significant increase in AQP4 mRNA expression. They hypothesized that these dysfunctional

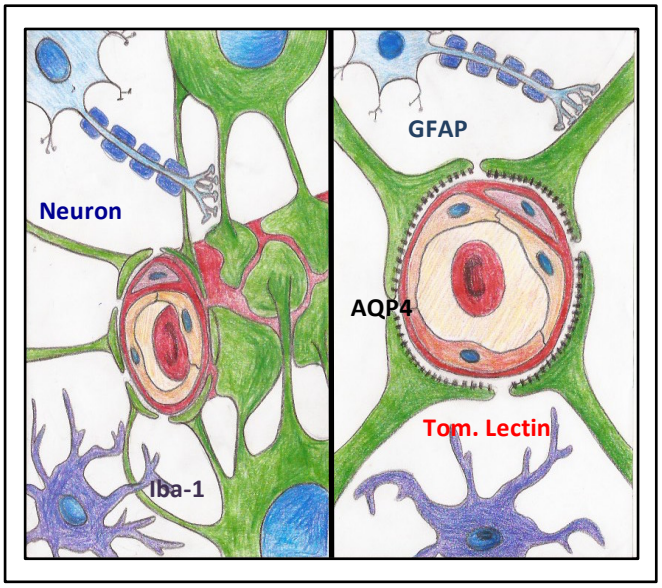

Figure 1: Depiction of the blood brain barrier including astrocytes (GFAP: glial fibrillary acidic protein - green), neurons (blue), aquaporin water channels (AQP4: Aquaporin 4 -black), microglia (Iba-1: Ionized Calcium-binding Adapter Molecule 1- purple), and vasculature (Tom. Lectin: Tomato Lectin - red)

astrocytes were releasing excessive amounts of the excitatory neurotransmitter glutamate, leading to hyperexcitability of neurons in spinothalamic pathways.

BBB/BSCB:

The BSCB is composed of capillary endothelial cells connected by tight junctions. The astrocytic endfeet abut the basal lamina and form the glial limitans (Figure 1). The BSCB functions to prevent the circulating blood from entering into the isolated environment of the CNS. It maintains this isolated environment by preventing the influx of large and/or hydrophilic molecules into the CNS, while allowing the entrance of small lipid soluble molecules. Permeability of the BSCB allows the entrance of peripheral immune cells into the parenchyma of the spinal cord, contributing to a toxic microenvironment that may disrupt functional recovery (Hansen et al., 2013). MMP-9 has also been implicated in BSCB dysfunction. Matrix metalloproteinases (MMPs) have a variety of

functions in the spinal cord, and can affect inflammation and BSCB functioning. MMP-9 contributes to the remote inflammatory microenvironment by increasing the permeability of the BSCB through degradation of the endothelial tight junctions. Activated astrocytes release MMP-3 by 24 h after injury, which then cleaves the pro-inflammatory form of MMP-9, leading to activation. Increased expression of MMP-9 has been observed as early as 7dpi and remains upregulated at 9 dpi in the lumbar cord (Hansen et al., 2013).

Breakdown of the BSCB could be one reason for the extravasation of peripheral immune cells into the lumber tissue. It could then be contributing to the pro-inflammatory microenvironment in this way. Our lab has also observed increased expression of pro-inflammatory TNFα in the lumbar enlargement 7d after SCI in mice (Hansen et al., 2013). Our lab has also shown BSCB permeability to Evans Blue Dye remote to a 9th thoracic segment (T9) contusion injury throughout the dorsal and intermediate grey matter within lumbosacral segments in mice by 7 dpi (Hansen et al., unpublished). The presence of remote BSCB breakdown and a pro-inflammatory microenvironment proved refractive to exercise-based therapies at early time points after injury, when neuroplasticity is postulated to be at its highest and is of increasing interest in promoting recovery after SCI (Hansen et al., 2013).

Opening of the BSCB has also been reported in uninjured mice in response to neuronal activity (Arima et al., 2012). Following electrical stimulation of the soleus muscle, Arima noted an inherent leakiness of the BSCB at L5 (Lumbar segment 5) where an influx of pathogenic CD4+ T cells into the CNS occurred via the dorsal blood vessels. This finding led to the belief that L5 is the 'gatekeeper' through which autoreactive T cells enter the spinal cord in experimental autoimmune encephalomyelitis (Arima et al., 2012). Dysfunction and/or opening of the BSCB barrier allows one avenue for the extravasation of peripheral immune cells into the CNS and may contribute to the toxic microenvironment observed in the lumbar cord in this way.

Hypothesis:

At chronic time points after a moderate contusive spinal cord injury, we hypothesize that there will be continuous dysfunction in the intermediate lumbar grey matter of the spinal cord. Additionally, we hypothesized that astrocytes would contribute to disturbances in fluid balance and cytotoxic edema through the up regulation of AQP4 channels along the endfeet, leading to swelling of these processes. Finally, we expected that active trafficking of peripheral immune cells would be shown through upregulation of ICAM1. Overall, we hypothesize that astrocytic dysfunction and increased expression of glial cells after thoracic injury would in fact be present in the lumbar cord.

Materials and Methods

Subjects and Surgeries:

Experiments were conducted in accordance with The Ohio State University Institutional Laboratory Animal Care and Use Committee. Adult (2 months) female C56BL/6J wild-type mice were obtained from the Jackson Laboratory. Mice were housed 3-4 per cage in a 12h light/dark cycle, and provided with food and water ad libitum. Laminectomy and spinal cord contusion injuries were performed as described previously (Jakeman et al., 2000; Kigerl et al, 2006, Hansen 2013). Briefly, mice were anesthetized with a mixture of ketamine (80 mg/kg) and xylazine (20 mg/kg) injected intraperitoneally and given prophylactic antibiotics (gentocin, 1 mg/kg) subcutaneously (subQ). Using aseptic techniques, the spinous process and lamina of T9 were removed to

expose the dura mater (Figure 2B). The vertebral column was stabilized with clamps in a stereotactic device at the T8 and T10 vertebral bodies and a moderate-severe contusion injury was induced by delivering a 75-kilodyne force injury using the Infinite Horizon Impactor (Precision Systems and Instrumentation, LLC, Fairfax Station, VA) (Figure 2A). The incision was closed in layers and 2 cc of sterile saline was provided subcutaneously to prevent dehydration. Mice received antibiotics (1 mg/kg gentocin, subQ) and saline for 5d after injury. Bladders were manually expressed twice per day until tissue was harvested (Hoschouer et al, 2010).

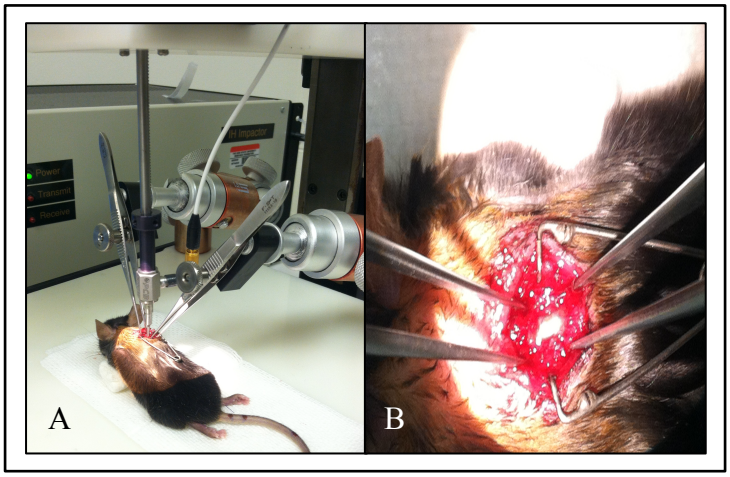

Figure 2A: Stereotactic device to stabilize animals for contusion injury
Figure 2B: Exposure of the dura mater above T9.

Deviations of force and displacement were analyzed in order to exclude biomechanical outliers of the injury (n=2). Animals (n=3) were also excluded based on health complications (ascites, n=1; eye prolapse, n=1; tooth caught in surgical staple, n=1). Open field locomotion was assessed at 1 dpi in order to screen for behavioral outliers using the Basso Mouse Scale (BMS) for Locomotion. Animals with a BMS score greater than 1.5 were removed from the study (n=2). Randomized group assignment and blinded BMS assessments occurred for all animals. Animals were also excluded from the study following tissue collection as some tissue was compromised due to improper storage (n=8).

Tissue Collection:

At previously determined endpoints, each animal was sacrificed by cardiac perfusion with 5 mL phosphate buffer (PB, pH 7.4), followed by 10 mL of paraformaldehyde (4%, pH 7.2) fixative. The animal was then perfused with 10 mL of Tomato Lectin (10ul/ml) to label the vasculature and finally 30 mL of paraformaldehyde. The remaining laminae of the vertebrae were removed and tissue was collected from the epicenter (5 mm on either side of the area of impact at T9), as well as the lumbar region spanning from L1 to the caudal end of the cord. All tissue was post-fixed in 4% paraformaldehyde for 4 hours and then rinsed for 24 h in 0.2M PB. Tissue was then cryoprotected in 30% sucrose, blocked in Tissue-Tek OCT compound (Optimal Cutting Temperature, Hatfield, PA) and then transversely sectioned at a 20 micrometer (μm) thickness on a Microm HM505E cyrostat (Electron Microscopy Sciences, Hatfield, PA). Naïve animals 22 and 23 were injected with the vascular tracer Evans Blue Dye, prior to sacrifice; however this was not quantified.

White Matter Sparing:

The lesion site was sectioned transversely at 20 um and stained for myelin to determine the lesion area and white matter sparing at the injury epicenter. Eriochrome cyanine (EC) staining, followed by differentiation with 5% iron alum and borax ferricyanide solutions, was performed as described previously (Basso et al., 2006; Kloos et al., 2005). The epicenter of the injury was determined as the section with the least amount of spared white matter and with the largest central lesion. Tissue was analyzed under light microscopy and converted to a computer image (MCID-Elite, Imaging Research, Ontario). A grid was positioned on each section randomly using Cavalerri estimator, and each point (p) was

assigned as white matter, grey matter, or lesion (Figure 3). For each area (dorsal/ventral/left/right), the point totals were added and converted to area as follows: estimated area = (ΣP) * (a/p) (ΣP is the sum of the points for an individual section; a/p is the area of each point) (Figure 3A). White matter sparing was compared to average LAM white matter, and lesion area was calculated compared to average section area of LAM controls. At this point, the 35 dpi timepoint was removed from the study due to a limited number of animals.

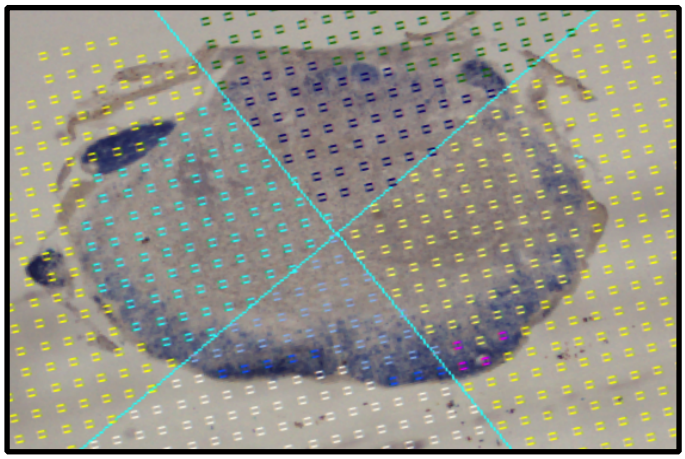

Figure 3: Grid analysis of white matter sparing and lesion area on a representative SCI image (35d timepoint)

Markers:

GFAP is an intermediated filament that is expressed by astrocytes, and is found to be upregulated in reactive astrocytes. Studies have shown that this protein is extremely important in the formation of a glial scar and in astrocytic reactivity (Sofroniew and Vinters, 2010). We evaluated GFAP expression in the lumbar cord from acute to chronic time points with the hypothesis that morphological indices of reactivity in astrocytes do not extend to chronic time points in the lumbar cord.

AQP4, which is found localized to the endfeet of astrocytes, is an integral membrane water channel protein that allows the conduction of water through the cell membrane. By examining the expression levels of AQP4 after SCI, evidence for continuous dysfunction in the astrocytes without the typical morphological activation seen early after injury is determined.

Tomato lectin was utilized to visualize the vascular endothelium of blood vessels supplying the cord. In order to determine if there was active trafficking of peripheral immune cells into the spinal cord, and whether this co-localized with the blood vessels, we also stained for the expression of intercellular adhesion molecule 1 (ICAM1). ICAM-1 is expressed on the inner surface of endothelial cells and can be induced by TNF-α, IL-1β, along with other products of reactive glial cells. ICAM-1 is also is involved in inflammation and T-cell mediated defenses (van de Stolpe and van der Saag. 1996).

The microglia/macrophage response was analyzed via staining for ionized calcium-binding adapter molecule-1 (Iba-1). Iba-1 is expressed on microglia and macrophages and was analyzed to determine microglia/macrophage morphology and expression.

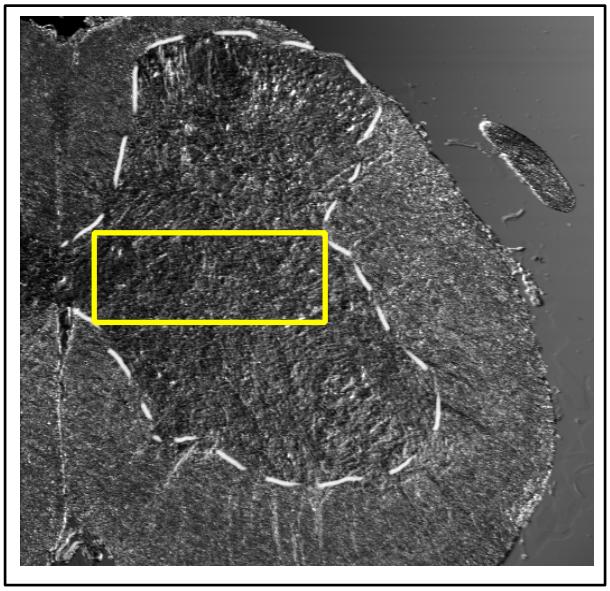

Figure 4: Example of box size determination for proportional area analysis measurements.

Histology:

Fluorescent immunohistochemistry was performed to examine astrocytes, microglia/macrophage reactivity and morphology, monocyte trafficking, and AQP4 channel expression. To investigate astrocytes a 1:7500 dilution of rabbit anti-GFAP antibody was utilized (Abcam ab7260). The antibody was incubated in blocking solution consisting of 4%BSA/0.1% Tx-100 in PBS overnight at room temperature. A goat-anti rabbit secondary which fluoresces at 488 nm was used at a dilution of 1:1000 in 4%BSA, 0.1% Tx-100 in PBS (AlexaFlour 488, ab150077). Microglia/macrophages were examined using a 1:200 dilution for rabbit anti Iba-1 prepared in blocking solution of 1%BSA/0.1%FG/3% NGS/0.2% Tx-100 in PBS. Incubation of the primary antibody occurred overnight at 4 degrees Celsius (Wako 019-19741). Iba-1 labeling was visualized with a goat anti-rabbit secondary at a 1:400 dilution (AlexaFlour 488, ab150077). The interface between vasculature and astrocytic end feet was visualized by staining for Aquaporin-4 water channels. A rabbit anti-AQP4 primary antibody was diluted at a concentration of 1:1000 in 10%NGS/0.3% Tx-100 and PBS (Chemicon AB3594). Slides were incubated in the primary overnight at room temperature. A goat anti-rabbit secondary was then used to visualize these water channels at a concentration of 1:200 in 10%NGS/0.3% Tx-100 and PBS (AlexaFlour 488, ab150077). ICAM-1 labeling was achieved by utilizing a goat anti-ICAM1 primary antibody at a concentration of 1:250 in blocking solution consisting of 1%BSA/3% NDS in PBS. The sections were incubated in the primary antibody overnight at 4 degrees Celsius (R&D Systems, AF796). ICAM-1 was then visualized with a donkey anti-goat secondary at a dilution of 1:250, which was incubated overnight at 4 degrees Celsius (Abcam 488, ab96935). For all stains, control sections incubated with primary and no secondary, and secondary and no primary were maintained in order to ensure positive labeling. All images were acquired using a Zeiss Laser Confocal Microscope (The Ohio State University Confocal Microscopy Imaging Facility). Images were taken at magnifications of 10x, 20x oil, 60x oil, and 120x oil.

Proportional Area Analysis:

Proportional area analysis was performed in lumbar cord sections in the intermediate zone of the grey matter stained for GFAP, ICAM1, Iba-1, and AQP4 (Figure 4A). The percent positive area was determined using ImageJ software (http://rsb.info.nih.gov/ij/) on confocal images. The starting point for the proportional area analysis was determined as the area above the central canal where the medial dorsal horn starts to ascend. A box was then created by extending laterally to the border between the grey and white matter, and then taken ventrally until it reached the medial border between the grey and whiter matter below the central canal (Figure 4). One intermediate box size was determined and used for all analyses

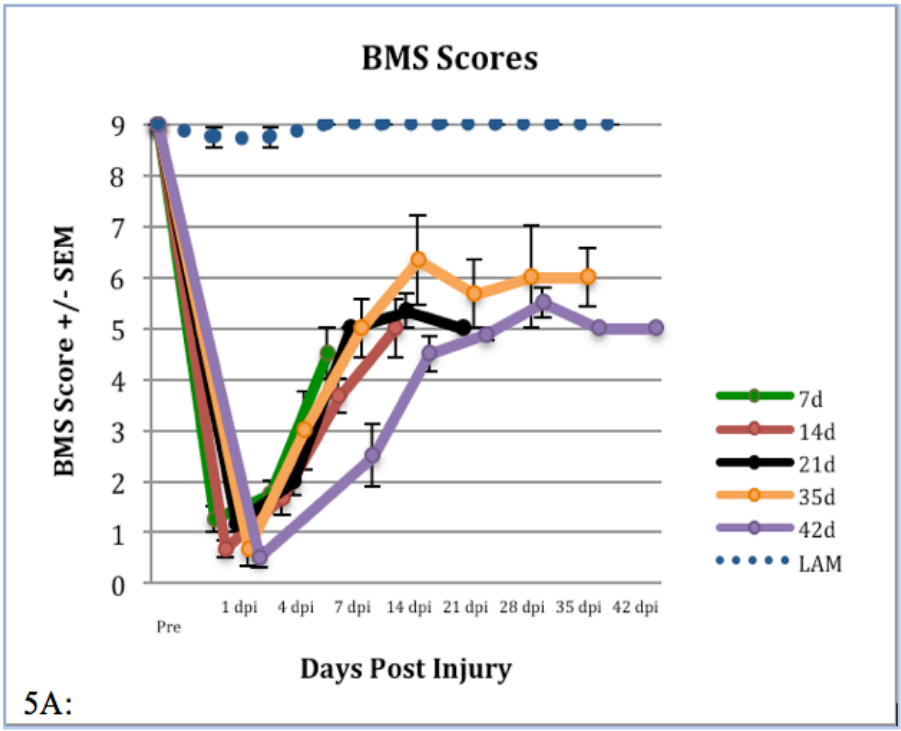

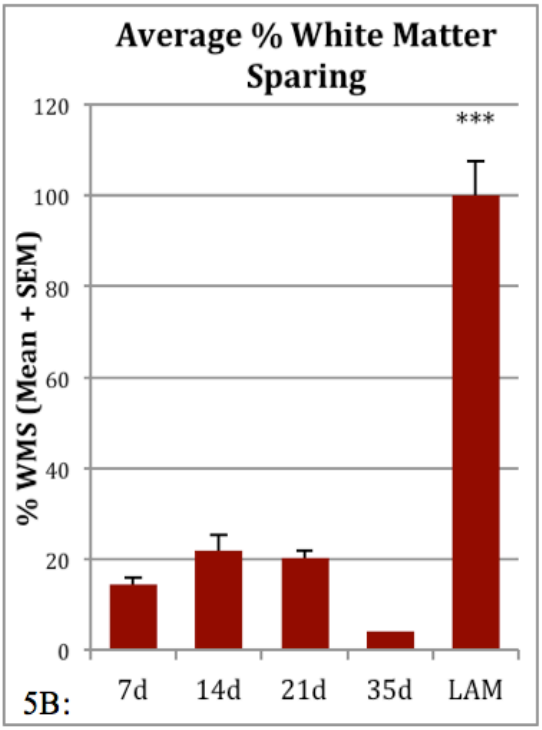

Injury severity and functional recovery was assured across all timepoints

Figure 5A: BMS scores were consistent across groups with no differences between SCI groups.

Figure 5B: %WMS was not significant across SCI groups, and only showed significance between SCI and LAM controls (*** $p < 0.001$).

Microglia Cell Body Size Measurements:

Microglia reactivity was determined by measurement of cell body size. Ten cell bodies per animal were assessed in the intermediate grey matter by systematically progressing through the image in a six-section grid to choose a representative sample of cell bodies to evaluate in the area of interest (Neurolucida). Cell body length and width were measured and multiplied to acquire average cell body area.

Locomotor assessments:

BMS scores in an open field were assessed to determine the extent of recovery after injury. Scores between 0 (no hindlimb movement) and 9 (normal locomotor function) were attributed to each animal after a four minute examination by two raters blinded to group assignment. Assessors determined movement of joints, weight-supported steps as well as plantar steps, trunk stability, and control of tail (Basso et al., 2006). Assessments were obtained at timepoints prior to the injury, 1dpi, 4dpi, 7dpi, and weekly thereafter until sacrifice.

Statistics:

White matter sparing, proportional area measurements, and microglia cell body size was analyzed using a One-way ANOVA with Tukeys post-hoc analysis. BMS scores were analyzed with repeated measures ANOVA with Tukeys post-hoc analysis.

Results

Lesion Severity:

BMS scores for all SCI timepoints showed a consistent response of injury and functional recovery among all timepoints compared to LAM controls (Figure 5A).

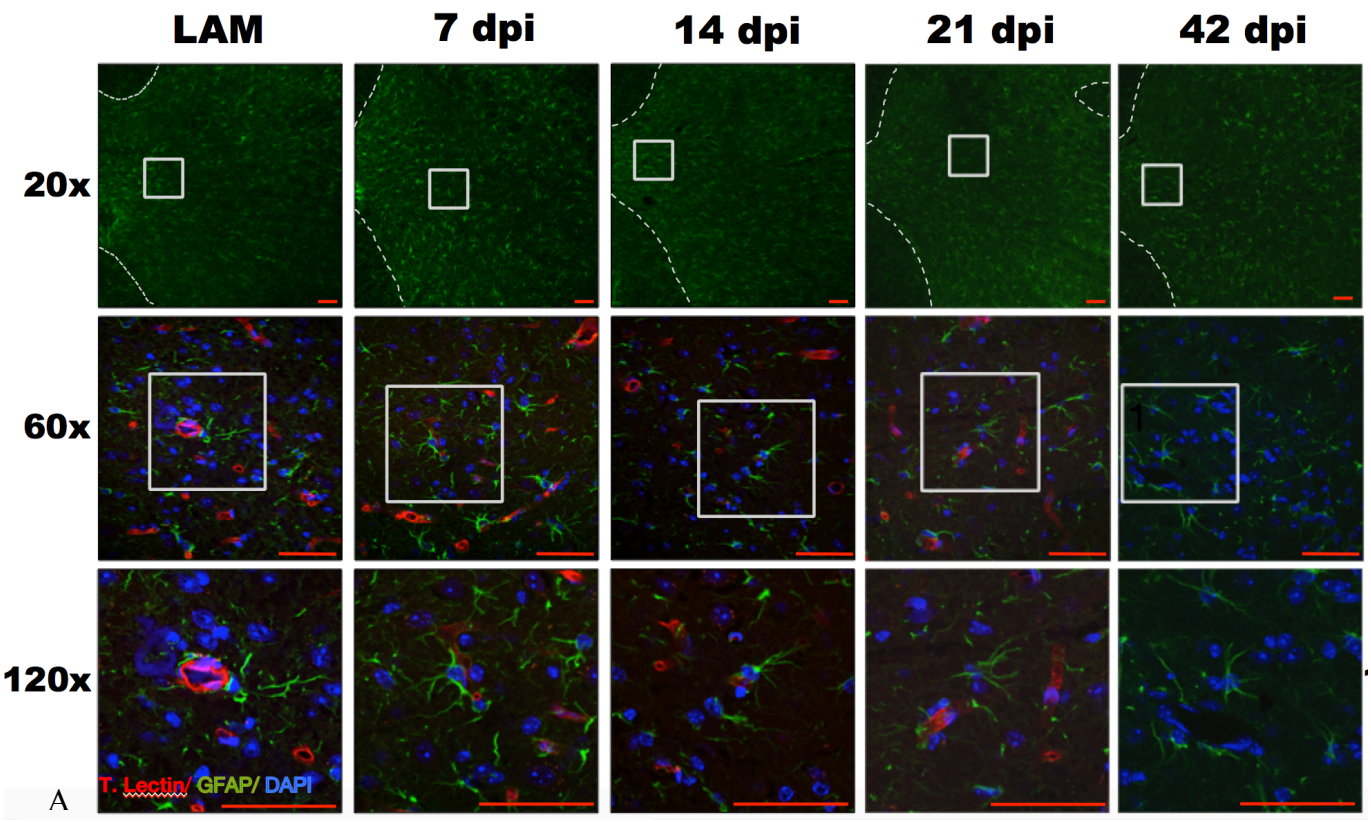

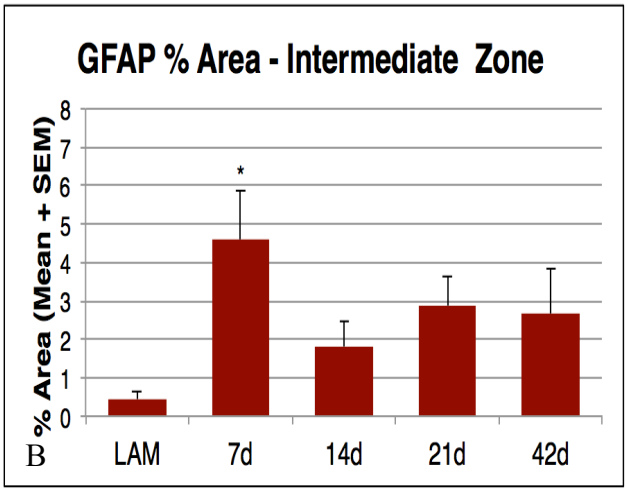

Astrocytes displayed increased expression in the intermediate grey matter at 7 dpi that continued at slightly increased levels through 42 dpi:
Figure 6A: Confocal images taken at various magnifications (20x, 60x, 120x) displaying upregulation of GFAP (green) and also labeled with tomato lectin (red), and DAPI (blue).
Figure 6B: Quantification of GFAP proportional area with significant upregulation seen at 7 dpi (* $p < 0.05$) that remained slightly increased out to 42 days after injury.
(All scale bars= 50 μm)

Animals showed an initial decrease in function indicating either no movement (0) or slight ankle movement (1) at 1 dpi. All SCI groups then showed a consistent functional recovery that did not differ significantly though 7 days after injury (7d = 4.5+/-0.5; 14d = 3.67+/-0.33; 21d = 5+/-0; 35d = 5+/-0.58; 42d = 2.5+/-0.61). Longer surviving SCI groups also plateaued at a similar BMS score by the time of sacrifice (average of 5-6 - indicates plantar stepping with no coordination (5) to some coordination (6)).

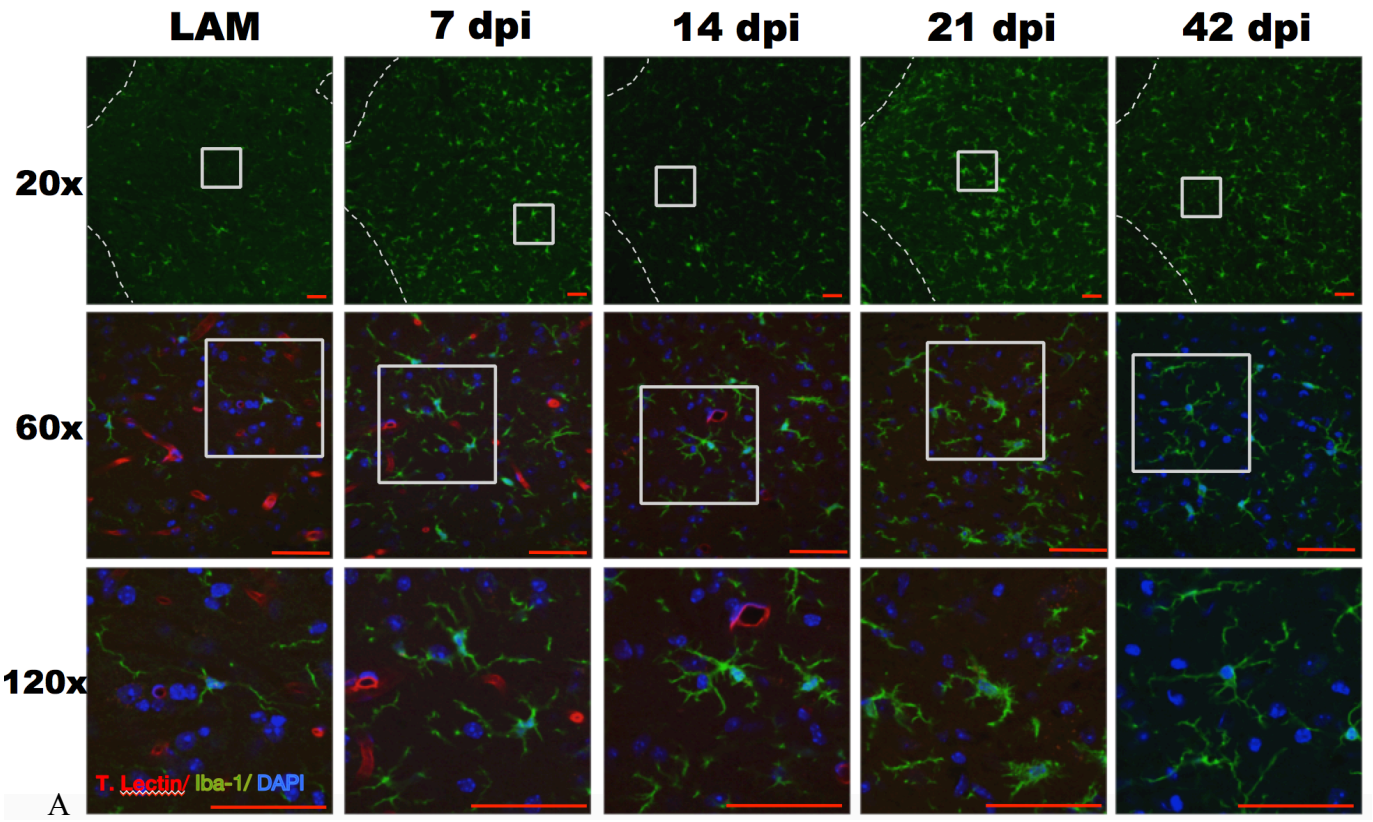

A

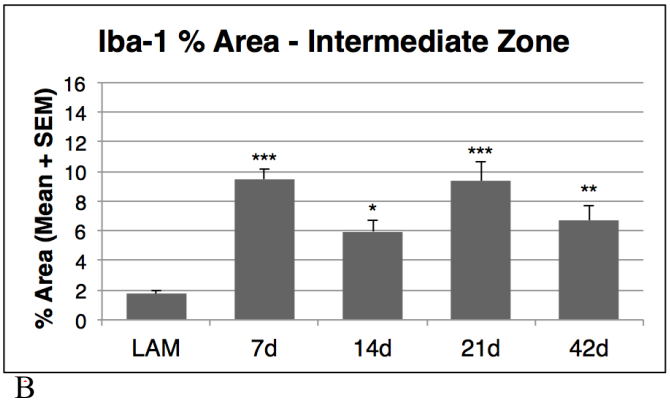

B

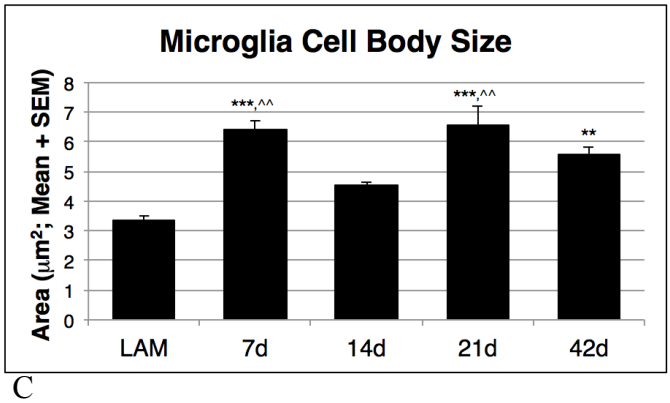

C

Microglia/macrophages displayed upregulation and a reactive phenotype:

Figure 7A: Panel displaying Confocal imaging of microglia/macrophages stained with Iba-1 (green), tomato lectin (red), and DAPI (blue).

Figure 7B: Quantification of PA measurements of Iba-1 showing a biphasic increase in expression with peaks at 7 and 21 dpi.

Figure 7C: Quantification of microglia/macrophage cell body size from 60x images showed a biphasic response and remained significantly upregulated at 42 dpi.

(*** $p < 0.001$; ** $p < 0.01$; * $p < 0.05$; ^^ $p < 0.01$)

All scale bars= 50 μm

Measurements of percent white matter sparing also confirmed a similar lesion severity between SCI timepoints. Average WMS ranged from 14-21% (7, 14, and 21d timepoints). SCI groups showed significantly less sparing compared to LAM controls. However, these were not different from each other, ensuring a moderate/severe injury across all SCI groups

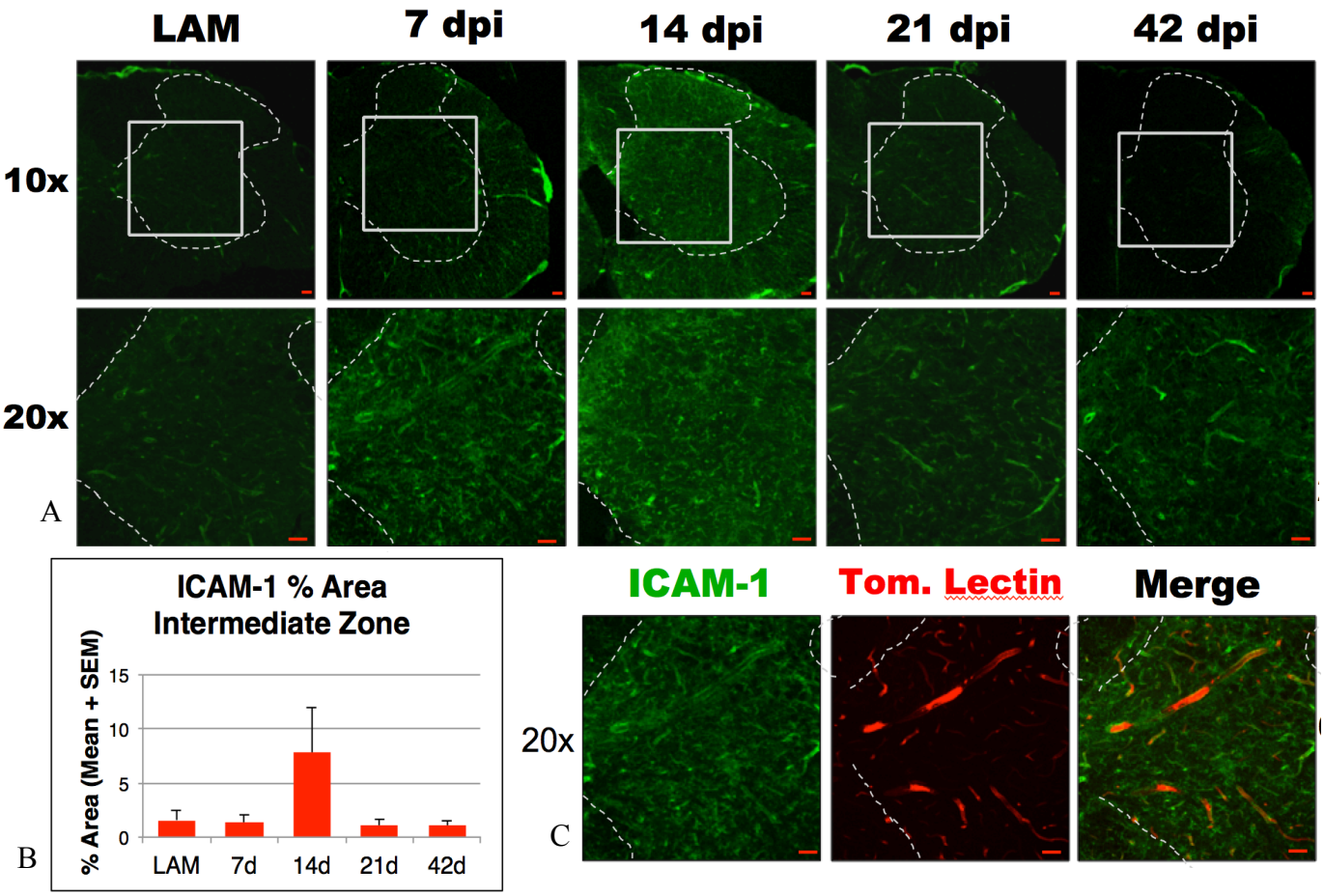

ICAM-1 displayed increased expression at 14 dpi that returned to baseline by 21 dpi
Figure 8A: Confocal imaging of ICAM-1 (green) expression that seemed to display a slight increase at 14 dpi.
Figure 8B: Quantification of ICAM-1 expression in the intermediate grey matter with highest upregulation at 14d (not significant).
Figure 8C: 20x magnification confocal images showing co-labeling of ICAM-1 and Tomato Lectin (Red) indicating potential active trafficking of peripheral immune cells into the lumbar spinal cord.

(One-Way ANOVA with Tukey's post hoc analysis, $p < 0.05$; LAM = 100% +/- 7.55; 7d = 14.30 +/- 1.55; 14d = 21.92 +/- 3.29; 21d = 20.16 +/- 1.69) (Figure 5B).

GFAP:

To determine the time course of astrocyte reactivity in the intermediate grey matter of the lumbar cord, proportional area analysis was assessed for GFAP (Figure 6A: top panel). Astrocytes at 7 dpi displayed a significantly increased expression of GFAP (LAM = 0.45 +/- 0.18; 7d = 4.58 +/- 1.26, $p < 0.05$). GFAP remained slightly upregulated through 42 dpi compared to LAM controls, however it was not significant (ranged from 1.81% at 14 dpi to 2.66% at 42 dpi) (Figure 6B). Astrocytic processes were visualized and displayed increased staining of processes (Green) and close localization with the vasculature (Red) (Figure 6A: middle and bottom panel).

Iba-1:

Microglia/macrophage reactivity was assessed via quantification of Iba-1 proportional area analysis in the intermediate

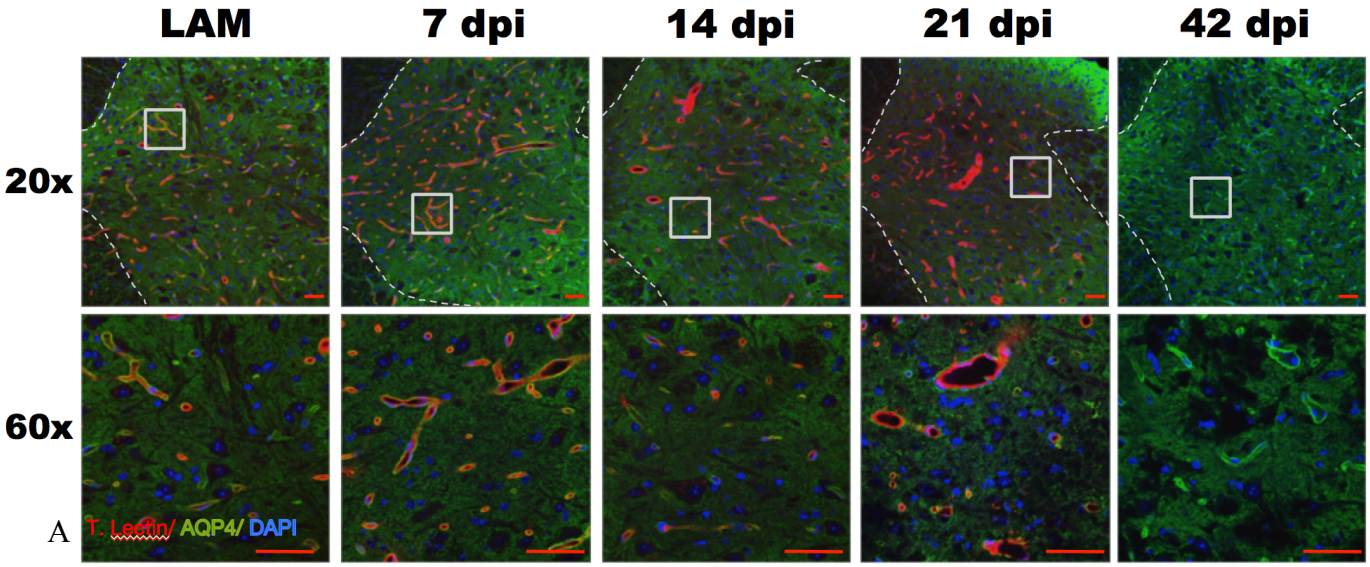

Aquaporin is seen to co-label with the vasculature

Figure 9: Increased co-labeling between blood vessels (red) and aquaporin water channels (green) was observed at 7d that seemed to decrease from 14 through 21 dpi.

grey matter (Figure 7A). A biphasic response with peaks at 7 dpi and 21 dpi was observed which remained upregulated at 42 dpi. Interestingly, there was a decrease in Iba-1 expression from 7 to 14 dpi that was not back to LAM control levels ((LAM = 1.73 +/- 0.20; 7d = 9.49 +/- 0.70; 21d = 9.35 +/- 1.34; $p < 0.000$; 14d = 5.96 +/- 0.75; $p < 0.05$; 42d = 6.72 +/- 0.99; $p < 0.01$). (Figure 7B).

Evaluation of microglia/macrophage activation was assessed via quantification of cell body area, and also demonstrated a biphasic response. Cell body size was observed to increase significantly at 7 and 21 dpi that continued at 42 dpi compared to LAM controls (LAM – 3.36 μm^2 +/- 0.16; 7d - 6.39 μm^2 +/- 0.31; 21d - 6.58 μm^2 +/- 0.61; $p < 0.000$; 42d - 5.60 μm^2 +/- 0.20; $p < 0.001$). Cell body size at 14 dpi was significantly decreased to control levels and was once again increased at 21 dpi (14d – 4.52 +/- 0.10; $p < 0.01$ (compared to 7d); $p < 0.005$ (compared to 21d) (Figure 7C).

ICAM-1:

Evaluation of active trafficking of peripheral immune cells into the lumbar microenvironment of the central nervous system was observed to increase slightly at 14 dpi (7.82% +/- 4.09, $p = 0.13$) but returned to baseline by 21 dpi through 42 dpi (Figure 8B) (No significance). Co-labeling of ICAM-1 and tomato lectin was observed indicating localization of this cell adhesion molecule to the vasculature (Figure 8C).

AQP4:

Confocal images taken in the intermediate grey matter of the lumbar cord (Figure 9) show increased co-labeling of the vasculature with AQP4 early. This co-localization appeared to be slightly elevated at 7 days after injury. From 14 through 21 dpi, this co-labeling along the blood vessels showed slightly less staining of aquaporin channels along the vasculature.

Discussion:

Increased expression of astrocytes and microglia/macrophage markers indicates a contribution of these glial cells after a spinal cord injury in the lumbar intermediate grey matter. The biphasic response seen in regards to microglia/macrophage expression and reactivity may indicate a secondary wave of inflammation being trafficked into the cord. These reactive glial cells can secrete pro-inflammatory cytokines that inhibit synaptic plasticity and learning, proving refractive to activity-based therapies (Hansen et al., 2013). Our lab has previously shown activation of microglia via assessments of cell body size and process retraction, along with increased expression of pro-inflammatory cytokines (Hansen et al., 2013; Detloff et al., 2008)

Our lab has previously shown that combination of behavioral treadmill training therapies with lessening of inflammatory activation through MMP-9 knockout mice increases functional recovery (Hansen et al., 2013). Task-specific treadmill training is capable of harnessing plasticity in locomotor networks to promote functional recovery, but this effect is dramatically reduced in the presence of a pro-inflammatory microenvironment. When plasticity is at its highest, in the early period after an injury, treadmill focused training can have a detrimental impact on return-of-function, theorized to be caused by an environment that proves refractive to these therapies (Hansen et al., 2013). We have shown, through knockout of MMP-9, that levels of TNFα remained reduced over the first week after injury that returned to baseline by 7 dpi. MMP-9 knock out animals had a more robust response to behavioral treadmill training as well. Microglia activation was also shown to be reduced at 7 dpi compared to wild type animals (Hansen et al., 2013). The production of pro-inflammatory cytokines by reactive glial cells in areas important for locomotor function, including CPG networks, can potentially impact efficacy of treadmill training therapies.

Comparison of BMS scores and the percent white matter sparing until animal sacrifice ensured a similar lesion severity across all SCI groups. At 1 dpi, the animals showed only slight ankle movements on average, indicating a similar severity of damage. As time passed, and spinal shock resolved, all groups showed a similar path of recovery that plateaued at the same level between groups. By the time of sacrifice, all animals showed on average plantar stepping without coordination, displaying a similar recover across groups and a similarity between injuries with no significance between groups (Basso et al., 2006). WMS between SCI groups was not significantly different, except when compared to LAM controls, further ensuring lesion severity and similarity.

Astrocytes exhibited significantly greater expression of GFAP at the 7-day timepoint that was reduced by 14 dpi which could indicate reduced activation in the lumbar cord at chronic timepoints. This up-regulation could be attributed to increased staining of processes, proliferation of astrocytes in the lumbar intermediate grey matter, or increased recruitment of reactive astrocytes into the environment caudal from the lesion. Confocal imaging seemed to support increased staining of astrocytic processes in the injured tissue, but more quantification of this must be performed in order to confirm. This upregulation of GFAP indicates that astrocytes are being affected at locations well away from the lesion site, and could be contributing to toxicity in the parenchyma of the spinal cord, and preventing plasticity and recovery. Pro-inflammatory cytokines like TNFα or IL-1β are produced in part by reactive astrocytes, and can prevent improvement in recovery from CPG - targeted therapies. Cell cycle proteins can activate astrocytes and it has been shown that using a cyclin-dependent kinase inhibitor can prevent the

activation of glial cells after injury, as well as the release of TNFα and IL-1β (Gwak et al., 2012). This shows that targeting TNFα and IL-1β, which can negatively impact locomotor recovery could increase the advantage of these behaviorally focused treatments.

Reactive astrocytes produce MMP-3, which breaks down collagen type IV, an essential component to maintenance of the integrity of the basil lamina of the BBB (Guertin, 2012). As astrocytes displayed the highest expression of GFAP at 7 days after injury, they could then be causing increased expression of ICAM-1 at 14 days after injury, as the MMP-3 helps to break down collagen type IV in the basil lamina. MMP-3 also cleaves the pro-inflammatory form of MMP-9, which is implicated in degrading the tight junctions between endothelial cells of the BSCB (Hansen et al., 2013). This process can be further elucidated by examining BSCB permeability after SCI in the lumber cord out to and past 14 dpi, to see if the potential for peripheral immune cells to enter the lumber parenchyma and contribute to aberrant plasticity is possible. Evaluating MMP-3 and MMP-9, as well as occludin, a tight junction marker between endothelial cells, and collagen type IV, could give us a better understanding of the role of astrocytes and microglia in breakdown of the BSCB, that then allows the entrance of peripheral cells into the isolated spinal cord that adds to an environment that does not respond well to activity based interventions.

The role of aquaporin water channels in disturbances of edema and the environment of the intermediate grey matter showed some increased co-labeling with tomato lectin early after injury in the lumbar cord, as well as decreased co-localization at later timepoints (14-21 dpi). The lack of AQP4 expression at the interface between the vessels and astrocytes at later timepoints could be attributed to proliferation of new processes or astrocytes that lack these water channels (Nesic et al., 2010). Further examination of aquaporin channels, and whether there is evidence of water dysregulation could provide greater insight into the role of astrocytes in dysfunction in the spinal cord. Quantification of the presence or absence of these channels localized to the blood vessels is needed to elucidate this role.

As microglia are the immune surveyors of the nervous system, they react quickly to an insult by retraction of their processes and hypertrophy of their cell bodies (Gwak et al., 2012). Iba-1 is a marker of microglia, as well as peripheral macrophages that are recruited into the nervous system. Microglia/macrophages were found to display a biphasic upregulation in Iba-1 from 7 through 42 dpi, with peak expression at 7 and 21 days after injury. This same response was seen when phenotype was evaluated, by determining the average cell body size at each timepoint. The biphasic response we observed may indicate a secondary wave of inflammation being trafficked into the lumbar parenchyma, and could be a potential target to reduce the toxicity associated with the products of these immune cells. Initially, microglia are activated soon after the injury and produce multiple cytokines and other chemicals that can then lead to recruitment of peripheral immune cells into the cord secondarily. By preventing this subsequent wave of inflammation, behavioral therapies may better harness the endogenous plasticity present in the cord without hindrance from a toxic microenvironment.

Further confirmation of microglial activation and pro-inflammatory cytokine production must be done. Previously, in the dorsal horn of the lumbar, our lab saw upregulation and reactivity of microglia out to 35 dpi and hypothesized their correlation with chronic neuropathic pain (Detloff et al., 2008). In the intermediate grey matter, reactive microglia/macrophages could be contributing to the development of spasticity after injury, in

which there is aberrant signaling from the alpha motor neuron that does not have any regulatory control from the upper motor neuron. More about their part in contributing to toxicity that prevents functional recovery must be elucidated, by determining whether these reactive microglia/macrophages are secreted inflammatory cytokines that could contribute to a noxious environment. Investigations of the presence of TNFα, IL-1β, MMPs, and other secretory factors of microglia, will be the next step to determine the effect they might have in this essential area of the spinal cord after an injury.

Trafficking of peripheral immune cells into the isolated environment of the CNS was evaluated using ICAM-1, and the highest proportional area was found at the 14 dpi timepoint. Although this was not significant, it showed an interesting relationship with the microglia and astrocyte response, as the highest percent proportional area for ICAM-1 was seen with the lowest microglial expression, and decreased reactivity as evaluated by a decrease in cell body size compared to 7 and 21-day SCI groups.

Additionally, using other markers of astrocytes, including S100β or glutamine synthetase, may be able to enhance the study of astrocytes following SCI. GFAP stains an intermediate filament present in astrocytes, but may not provide a full picture of astrocytic reactivity. Determination of whether astrocytes are proliferating or if there is increased staining of finely branching processes and the extent of this branching and the cell bodies are not determinable through GFAP staining, and can lead to underestimation of astrocytic presence (Sofroniew and Vinters, 2010).

Conclusion:

In conclusion, we discovered activation of glial cells in locomotor regions of the lumbar spinal cord involved in CPG functioning and in interneuronal communication within the intermediate grey matter that continued at some level through chronic timepoints. Based on our previous findings, it is likely that these reactive microglia/macrophages and astrocytes are contributing to a toxic microenvironment through the production of inflammatory cytokines and products that serve to breakdown the BSCB, thus allowing trafficking of peripheral cells in the spinal cord. This secondary inflammatory response in the lumbar microenvironment proves refractive to activity-based therapies and prevents functional recovery after an injury. The biphasic response seen with staining of Iba-1 and increased microglia/macrophage cell body size may indicate a secondary wave of inflammation, potentially being trafficked in from the periphery that negatively impacts plasticity in the cord. Further investigation into the role of these products of reactive glial cells, and their role in breakdown of the BSCB, may provide a therapeutic target for improving outcomes using behavioral treatments. More information and quantification of the role of aquaporin water channels in this toxic microenvironment could further elucidate their role in dysfunction as well. Overall, astrocytes and microglia displayed upregulation of markers indicating reactivity. Further study of how they are contributing to toxicity in the lumber parenchyma may allow locomotor therapies to harness the natural plasticity present after an injury, improving functional recovery.

Acknowledgements:

I would like to thank D. Michele Basso, PT, Ed.D; Timothy D. Faw, PT, DPT, NCS; Samantha D. Kerr; Lesley C. Fisher; Rochelle Deibert; and Kathleen Kisseberth for all of their help and support in the completion of this project.

References:

Ahn SN, Guu JJ, Tobin AJ, Edgerton VR, Tillakaratne NJK. Use of c-fos to Identify Activity-Dependent Spinal Neurons After Stepping in Intact Adult Rats. Spinal Cord 2006; 44:547-559.

Arima Y, Harada M, Kamimura D, Park JH, Kawana F, Yull FE, Kawamoto T, Iwakura Y, Betz UAK, Marquez G, Blackwell TS, Ohira Y, Hirano T, Murakami M. Regional Neural Activation Defines a Gateway for Autoreactive T Cells to Cross the Blood-Brain Barrier. Cell 2012; 148:447-457.

Bareyre FM, Schwab ME: Inflammation, Degeneration, and Regeneration in the Injured Spinal Cord Insights from DNA Microarrays. TRENDS in Neuroscience 2003; 26;555-563.

Basso DM, Fisher LC, Anderson AJ, Jakeman LB, McTigue DM, Popovich PG: Basso Mouse Scale for Locomotion Detects Differences in Recovery after Spinal Cord Injury in Five Common Mouse Strains. J Neurotrauma 2006; 23:5635-59.

Detloff MR, Fisher LC, McGaughy V, Longbrake EE, Popovich PG, Basso DM: Remote Activation of Microglia and Pro-inflammatory Cytokines Predict the Onset and Severity of Below-Level Neuropathic Pain after Spinal Cord Injury in Rats. Experimental Neurology 2008; 212:337-347.

Francesca B, Rezzani R: Aquaporin and Blood Brain Barrier. Current Neuropharmacology 2010; 8:92-96.

Greenhalgh AD and David S: Differences in the Phogytic Response of Microglia and Peripheral Macrophages after Spinal Cord Injury and Its Effects on Cell Death. J Neuroscience 2014; 34(18)-6316-6322.

Guertin PA: Central Pattern Generator for Locomotion: Anatomical, Physiological, and Pathophysiological Considerations. Front Neurol 2012; 3(183):1-15.

Gwak YS, Kang J, Unabia GC, Hulsebosch CE: Spatial and Temporal Activation of Spinal Glial Cells: Role of Gliopathy in Central Neuropathic Pain Following Spinal Cord Injury in Rats. Exp, Neurology 2012; 234(2):362-372.

Hansen CN, Fisher LC, Deibert RJ, Jakeman LB, Zhang H, Noble-Haesslein L, White S, Basso DM: Elevated MMP-9 in the Lumbar Cord Early after Thoracic Spinal Cord Injury Impedes Motor Relearning in Mice. J Neuroscience 2013; 33(32):13101-13111.

Hansen CN, Kerr SC, Deibert RJ, Wohleb E, Godbout J, Sheridan J, Basso DM. Activity-Dependent Myeloid Trafficking in Lumbar Locomotor Networks after Thoracic SCI.
Chimera Manuscript- Hansen et al, unpublished

Hoschouer EL, Basso DM, Jakeman LB. Aberrant sensory responses are dependent on lesion severity after spinal cord contusion injury in mice. Pain 2010;148:328–342.

Jakeman LB, Guan Z, Wei P, Ponnappan R, Dzwonczyk R, Popovich PG, and Stokes BT: Traumatic spinal cord injury produced by controlled contusion in mouse. J.

Neurotrauma 2000; 17:299–319.

Kigerl KA, McGaughy VM, Popovich PG: Comparative analysis of lesion development and intraspinal inflammation in four strains of mice following spinal contusion injury. J Comp Neurol 2006; 494:578–594.

Kjaerulff O, Kiehn O. Distribution of Networks Generating and Coordinating Locomotor Activity in the Neonatal Rat Spinal Cord in Vitro: A Lesion Study. J Neuroscience 1996; 16(18):5777-5794.

Kloos AD, Fisher LC, Detloff MR, Hassenzahl DL, Basso DM: Stepwise motor and all-or-none Sensory Recovery is Associated with Nonlinear Sparing After Incremental spinal Cord Injury in Rats. Experimental Neurology 2005; 191:251-265.

Kwon BK, Tetzlaff W, Grauer JN, Beiner J, Vaccaro AR: Pathophysiology and pharmacologic treatment of acute spinal cord injury. The Spine Journal 2004; 4:451-464.

Mautes AEM, Weinzierl MR, Donovan F, Noble LJ : Vascular Events After Spinal Cord Injury : Contribution to Secondary Pathogenesis. Physical Therapy 2000; 80:673-687.

Nesic O, Guest JD, Zivadinovic D, Narayana PA, Herrera JJ, Grill RJ, Mokkapati VUL, Gelman BB, Lee J. Aquaporins in Spinal Cord Injury: The Janus Face of Aquaporin 4. J Neuroscience 2010; 168:1019-1035.

Nesic O, Lee J, Johnson KM, Ye Z, Xu G, Unabia GC, Wood TG, McAdoo DJ, Westlund KN, Hulsebosch CE, Perez-Polo JR. Transcriptional Profiling of Spinal Cord Injury-Induced Central Neuropathic Pain. J Neurochemistry 2005; 95:998-1014.

Nesic O, Lee J, Ye Z, Xu G, Unabia GC, Rafati D, Hulsebosch CE, Perez-Polo JR: Acute and Chronic Changes in Aquaporin 4 Expression After Spinal Cord Injury. Neuroscience 2006; 143:779-792.

Popovich PG, Hickey WF: Bone Marrow Chimeric Rats Reveal the Unique Distribution of Resident and Recruited Macrophages in the Contused Rat Spinal Cord. Journal of Neuropathology and Experimental Neurology 2001; 60:676-685

Popovich PG, Horner PJ, Mullin BB, Stokes BT: A Quantitative Spatial Analysis of the Blood-Spinal Cord Barrier. Experimental Neurology 1996; 142:258-275.

Sandler AN, Tator CH: Regional Spinal Cord Blood Flow in Primates. J Neurosurgery 1976; 45:647-659.

Sofroniew MV, Vinters HV: Astrocytes: Biology and Pathology. Acta Neuropathology 2010; 119:7-35.

Spinal Cord Injury: Facts and Figures at a Glance." The National SCI Statistical Center, Aug. 2014. <https://www.nscisc.uab.edu/PublicDocuments/fact_figures_docs/Facts 2014.pdf>.

"Spinal Cord Injury: Hope Through Research." National Institute of Neurological Disorders and Stroke (NINDS), 23 Feb. 2015. <http://www.ninds.nih.gov/disorders/sci/detail_sci.htm>.

van de Stolpe A, van der Saag: Intercellular adhesion molecule-1.
J Mol Med 1996; 74:13–33